

Investigating the Role of Inflammatory Response in Polycystic Ovary Syndrome Using Integrated RNA-Seq Analysis

Lei Liu^{1,*}, Shanshan Liu^{2,*}, Fuyan Bai¹, Yangxin Deng¹, Xinhuan Zhang¹, Li Wang³

¹Department of Endocrinology, the Second Affiliated Hospital of Shandong First Medical University, Taian, Shandong, People's Republic of China;

²General Gynecology, the Tai'an Central Hospital, Taian, Shandong, People's Republic of China; ³Department of Pharmacy, the Second Affiliated Hospital of Shandong First Medical University, Taian, Shandong, People's Republic of China

*These authors contributed equally to this work

Correspondence: Xinhuan Zhang; Li Wang, Email zhangxh22009@126.com; suxinlan1027@126.com

Background: An important factor in the pathogenesis of polycystic ovary syndrome (PCOS) is chronic low-grade inflammation. However, the exact pathophysiology of PCOS is currently unknown, which makes clinical diagnosis and the development of effective treatments more difficult. We aimed to investigate the role of the inflammatory response in initiating and progressing PCOS.

Methods: 13 control granulosa cell samples and 15 granulosa cell samples from patients with PCOS were obtained from the GSE102293, GSE34526, and GSE5850 datasets. The gene set variation analysis (GSVA) method was used to calculate the inflammatory response score. Subsequently, the genes associated with inflammation in the hub were identified using differential expression analysis and weighted gene co-expression network analysis (WGCNA). The findings were confirmed by analysis of independent datasets and examination of clinical samples by qRT-PCR analysis. A consensus cluster analysis was conducted to categorize the PCOS samples into subtypes related to inflammation. Functional enrichment and analysis of immune cell infiltration were conducted to explore the potential mechanisms involved. Additionally, the CMap database was utilized to predict potential drugs, and the results were confirmed through molecular docking.

Results: During the training cohort analysis, we identified five distinct genes (TGFB2, ICAM3, WIPF1, SLC11A1, and NCF2) that could serve as potential diagnostic markers for PCOS. The expression levels of these genes were confirmed through validation in both the test set and clinical samples. In training cohort, two distinct inflammatory patterns (C1 and C2) were identified, and the C2 subtype exhibited activated immune- and inflammation-related pathways. Esmolol was shown to have potential as a drug to treat PCOS and it showed good results for molecular binding at TGFB2, ICAM3, WIPF1, SLC11A1, and NCF2 proteins.

Conclusion: Five diagnostic biomarkers and two inflammation-related molecular types associated with PCOS were identified, and esmolol was a potential drug for PCOS treatment. Our findings provided new diagnostic markers and potential small-molecule drugs for PCOS diagnosis and prevention.

Keywords: polycystic ovary syndrome, inflammatory response, diagnostic biomarkers, molecular subtypes, esmolol

Introduction

Polycystic ovary syndrome (PCOS), which is typically characterized by polycystic ovaries, anovulation, and hirsutism, is a common female endocrine disease.¹ It is a major cause of low female fertility, affecting approximately 4–18% of the total population.² PCOS is also a significant risk factor for metabolic and cardiovascular sequelae, often associated with obesity, dyslipidemia, and insulin resistance.³ At present, the Rotterdam criteria and clinical symptoms are the main diagnostic criteria of PCOS.⁴ So far, no effective diagnostic biomarkers or treatments exist for PCOS patients.^{5,6} The evidence to date suggests that PCOS may be a complex disease that is influenced by the environment, epigenetic variants, and genetic factors.⁷ However, the precise pathogenesis of PCOS remains unclear. A better comprehension of the pathogenesis of PCOS could lead to enhancements in clinical diagnosis, treatment, and reproductive outcomes.

A recent study has shown that inflammation is implicated in ovulation and is key to follicular dynamics.⁸ In particular, women with PCOS are more likely to be overweight. The development of inflammation is linked to visceral adipose tissue. An inflammatory response is generated in visceral adipose tissue mainly by increased monocyte chemotactic proteins, secretion of inflammatory factors, and recruitment of immune cells to maintain the inflammatory state of adipocytes.⁹ Thus, PCOS may be associated with inflammatory cytokines and a low-grade inflammation state. A previous study has revealed that inflammation in PCOS may be in part dependent on visceral fat tissue.¹⁰ In addition, the peripheral blood of PCOS patients was found to have significantly elevated inflammatory cytokines, adipokines, and their paralogs.¹¹ A lipid-induced pro-inflammatory state may underlie hyperandrogenaemia, dyslipidemia, and insulin resistance in patients with PCOS.¹² It has been shown that obese PCOS groups have a higher expression of NF- κ B p65 in the endometrium, which is associated with increased insulin resistance.¹³ Furthermore, women with PCOS have increased NF- κ B activation and TNF- α expression.¹⁴ However, the role of inflammatory response in the pathogenesis of PCOS has rarely been investigated. Therefore, the investigation of the factors involved in the inflammatory response that leads to the development and progression of PCOS may provide a greater understanding of PCOS and theoretical guidance to improve the clinical diagnosis and treatment of PCOS.

In this study, we downloaded the PCOS-associated datasets from Gene Expression Omnibus (GEO) database. Hub inflammatory response-related genes were identified by WGCNA. We carried out consensus clustering analysis, enrichment analysis, and immune cell infiltration analysis of PCOS samples based on differentially expressed inflammation-related genes. Furthermore, based on the results of differentially expressed analysis, the prediction of potential drugs for the treatment of PCOS was performed and the possible mechanism of action was verified using the molecular docking method. Our findings provided a theoretical basis to better understand inflammation in PCOS pathogenesis. Figure 1 showed the flow chart of the present study.

Methods and Materials

Data Acquisition and Preprocessing

A total of six PCOS-related datasets are downloaded from the GEO database (Table 1). The GSE102293 dataset contained four control samples and two PCOS samples; the GSE34526 dataset consisted of three control samples and seven PCOS samples; the GSE5850 dataset consisted of twelve samples, of which six were from the control group and six were from the disease group. All samples were derived from granulosa cells. We then used the “sva” and “gcrma” R packages to combine and normalize these three datasets into a testing dataset. In addition, there are three independent

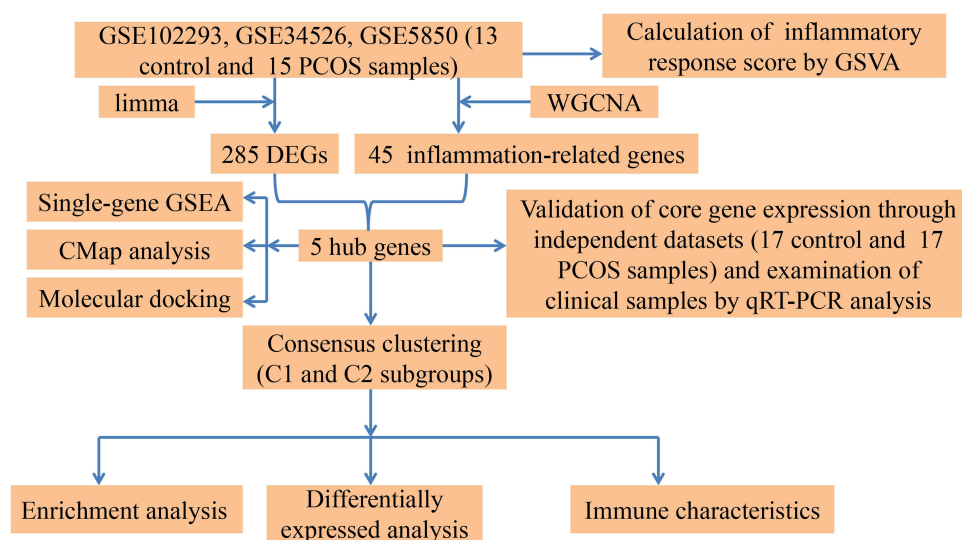


Figure 1 The workflow of the present study.

Table I The Information of PCOS-Related Datasets

GEO ID	Platform	Control Group	Disease Group	Source	Application
GSE102293	GPL570	4	2	Granulosa cells	Training set
GSE34526	GPL570	3	7	Granulosa cells	Training set
GSE5850	GPL570	6	6	Granulosa cells	Training set
GSE137684	GPL17077	4	8	Granulosa cells	Test set
GSE80432	GPL6244	10	6	Granulosa cells	Test set
GSE114419	GPL17586	3	3	Granulosa cells	Test set

datasets (GSE137684, GSE80432, and GSE114419 datasets) that have been merged and normalized by the “sva” and “gcRma” R packages and used as validation datasets.

Identification of Differentially Expressed Genes (DEGs) and Functional Enrichment Analysis

The DEGs between the control and PCOS groups were identified using the “limma” package. The thresholds for implementing the differentially expressed analysis were $p\text{-value} < 0.01$ and $|\log \text{fold change (FC)}| \geq 0.5$. The “pheatmap” package was used to visualize the results of DEGs. The “ggplot2” was used to map the volcano plot. Metascape (<http://metascape.org/>) is an online analytics platform that provides biologists with a comprehensive resource for annotating and analyzing gene lists.¹⁵ To investigate the biological functions and pathways of DEGs, GO and KEGG enrichment analyses were performed using Metascape.

Gene Set Enrichment Analysis (GSEA)

GSEA was performed for the identification of the most significant pathways between the molecular subgroups.¹⁶ ClusterProfiler package was applied for GSEA. To assess relevant pathways and molecular mechanisms, the “h.all.v7.4.symbols.gmt” subset was downloaded from the Molecular Signatures Database. $P \text{ value} < 0.05$ was considered statistically significant.

Assessment of Inflammatory Response Score

The inflammatory response score was assessed by using GSVA. We downloaded the “h.all.v7.4.symbols.gmt” subset from the Molecular Signatures Database. Then, the inflammatory response score was calculated for each sample in the inflammatory response gene set using the GSVA package based on the gene expression profile of the testing set. The inflammatory response score matrix was obtained, and the result was visualized by a boxplot.

Weighted Gene Co-Expression Network Analysis (WGCNA)

Using gene expression profiling, we calculated the Median Absolute Deviation (MAD) for each gene separately, removing the top 50% of genes with the lowest MAD. Then, the outlier genes and samples were removed using the goodSamplesGenes method of the WGCNA package, and a scale-free co-expression network was further constructed using WGCNA. Genes with high connectivity in the inflammatory response score module were identified as hub genes based on the cut-off criteria (Module membership > 0.8 and Gene significance > 0.8).

Protein-Protein Interaction (PPI) Network Analysis

In this study, we constructed the protein-protein interaction (PPI) network using the STRING database (<http://www.string-db.org/>) to identify co-expressed genes that are highly associated with the inflammatory response.¹⁷ The PPI network was then visualized and analyzed using Cytoscape software (<http://cytoscape.org/>, version 3.7.2).¹⁸ Finally, we performed topological analysis on the PPI network, calculating the degree of each gene to determine their importance. Genes with higher degrees were considered to be more important in the network.

Single Gene GSEA

For single gene GSEA, we used GSEA software to classify samples into high and low expression groups based on the median values of gene expression levels. The “c2.cp.kegg.v7.4.symbols.gmt” subset was downloaded from the Molecular Signatures Database to assess the relevant molecular mechanisms of genes based on gene expression profile and phenotypic grouping.

Consensus Clustering Analysis

The ConsensusClusterPlus package was used to perform a consensus clustering analysis based on the gene expression profile of inflammatory response score-related genes. Subsequently, the PCOS samples were classified into various subtypes.

Quantification of Immune Cell Abundance

CIBERSORT is a tool for the estimation of the abundance of member cell types in mixed cell populations based on gene expression data.¹⁹ We used the CIBERSORT to gain access to the subsets of immune cells in the molecular subtypes. The results were visualized using the “ggplot2” package.

Samples Collection and Quantitative Real-Time Polymerase Chain Reaction (qRT-PCR) Analysis

Between 2021 and 2022, we enrolled 16 women who had undergone in vitro fertilization and embryo transfer at the Second Affiliated Hospital of Shandong First Medical University to collect ovarian granulosa cells. According to the Rotterdam criteria, 8 patients were diagnosed with PCOS due to the presence of polycystic ovaries, hyperandrogenism, oligoovulation, and anovulation.²⁰ Subjects who had tumors that secreted androgens, Cushing’s syndrome, congenital adrenal hyperplasia, endometriosis or chronic metabolic disease were not included in the study. The control group comprised 8 patients who underwent in vitro fertilization treatment for tubal disease. These patients exhibited normal ovarian morphology, regular menstrual cycles, and normal hormone levels. All individuals who took part in this study were below 40 years old. The Ethics Committee of the Second Affiliated Hospital of Shandong First Medical University granted approval for this study, and all participants provided informed consent.

Cumulus-oocyte complexes were harvested using ultrasound-assisted vaginal puncture and subsequently rinsed in a solution of phosphate-buffered saline. Granulosa cells were then carefully extracted from the cumulus-oocyte complexes. The granulosa cells were subjected to RNA extraction using TRIzol Reagent (ThermoFisher Scientific, USA) according to the manufacturer’s instructions to obtain total RNA. The purified RNA was then used for cDNA synthesis using cDNA synthesis kits (Invitrogen, USA). The qRT-PCR analysis was carried out on the ABI ViiA 7 Real-time PCR system (Applied Biosystems, USA). β -actin was used as a reference gene. The relative mRNA expression levels were determined using the $2^{-\Delta\Delta C_t}$ method. The primer details were presented in [Table S1](#).

Candidate Drugs Identification and Molecular Docking Analysis

Connectivity Map (CMap) (<https://clue.io/data>), is a prediction tool used to screen potential compounds for their ability to activate or inhibit pre-specified genes.²¹ In addition, the CMap query provides indicators of similarity between perturbed genes and up- or down-regulated genes to enable comparison between drug-induced gene profile and gene expression profile.²² A score lower than 0 means that the changes induced by the drugs are different from those caused by the uploaded genes, which indicates that the drug may exert some therapeutic effects against the disease. A connectivity score of < -95 is considered a viable prediction for small molecule compounds.²³ In the present study, we uploaded DEGs from the normal and disease groups into the CMap database to identify small molecule drugs that may inhibit the biological progression of PCOS. The structure of proteins was downloaded from Protein Data Bank (PDB) database (<https://www.rcsb.org>). The structure of small molecule drugs was downloaded from the PubChem database (<https://pubchem.ncbi.nlm.nih.gov/>). The molecular docking analysis was performed using AutoDock (version 1.5.7), and the results were visualized using PyMOL software.

Statistical Analysis

The bioinformatics data was analyzed and visualized using R software version 4.2.1. GraphPad Prism 8.0 software was employed to analyze the experimental data. The results were represented as the average value along with the standard deviation (SD). Group comparisons were conducted with a *t*-test, with statistical significance denoted by a *p*-value less than 0.05.

Results

Identification of DEGs and Functional Enrichment Analysis

From the UMAP plot we can observe that before the removal of the batch effect the samples from each dataset are clustered together individually, suggesting a batch effect ([Figures S1A](#) and [S2A](#)), and after the removal of the batch effect the samples from each dataset are clustered and intertwined with each other, suggesting a better removal of the batch effect ([Figures S1B](#) and [S2B](#)). As per the Rotterdam criteria, 32 patients were identified with PCOS. The training set, comprising of merged GSE102293, GSE34526, and GSE5850 datasets, included 28 samples (13 from the control group and 15 from the PCOS group), while the test set, consisting of merged GSE137684, GSE80432, and GSE114419 datasets, comprised of 34 samples (17 from the control group and 17 from the PCOS group). All samples were obtained from granulosa cells.

As presented in the volcano map ([Figure 2A](#)) and heatmap ([Figure 2B](#)), the training set was screened for 285 DEGs using the “limma” package, with 149 genes down-regulated and 136 genes up-regulated, based on a *p*-value < 0.01 and |log fold change (FC)| ≥ 0.5 ([Table S2](#)). In addition, we performed the functional enrichment analysis to investigate the potential biological functions of DEGs. The Results revealed that the DEGs were significantly enriched in inflammation- and immune-related pathways, such as leukocyte activation, positive regulation of cytokine production, immune response-activating signaling pathway, inflammasomes, negative thymic T cell selection, positive regulation of NF-kappaB transcription factor activity, etc ([Figure 2C](#) and [D](#)). Furthermore, the significantly enriched pathways in the PCOS group were IL6-JAK-STAT3 signaling (ES = -0.61, *p* = 0.008), IL2-STAT5 signaling (ES = -0.42, *p* = 0.011), inflammatory response (ES = -0.55, *p* = 0.02), apoptosis (ES = -0.41, *p* = 0.03), and P53 pathway (ES = -0.38, *p* = 0.048), based on the “h.all.v7.4.symbols.gmt” gene set ([Figure 3A](#)). To further validate the GSEA results, we calculated the inflammatory response score in the control and PCOS groups using the GSVA algorithm. Compared to the control group, the inflammatory response score was significantly increased in the PCOS group (*p* < 0.05, [Figure 3B](#)). All these findings implied that the inflammatory response may play an important role in the development of PCOS. Thus, we selected it as the subject of our study.

Identification of Inflammatory Response Score-Related Modules by WGCNA

To further identify key genes associated with inflammatory score, we performed WGCNA analysis. A total of 20521 genes in the training set were used for WGCNA analysis. As shown in [Figure 3C](#), 21 gene modules were identified by WGCNA. Among these modules, the turquoise (*r* = 0.82, *p* = 0) and pink (*r* = 0.81, *p* = 0) modules exhibited a significant correlation with inflammatory response scores ([Figure S3](#)). For further analysis, 45 hub genes were identified in the turquoise and pink modules ([Table S3](#)).

PPI and Enrichment Analyses Were Conducted on the Genes Identified from the Hub Modules of the WGCNA

A PPI network was constructed using 45 genes identified in the String database. To streamline the analysis, nodes with fewer edges in the PPI network were removed, resulting in a final set of 31 nodes ([Figure S4A](#)). We conducted functional enrichment analysis on these genes, revealing their significant involvement in various biological processes. Specifically, our results demonstrated that these genes were primarily associated with phagocytosis, fc-gamma receptor signaling pathway, myeloid leukocyte activation, phagosome, neutrophil extracellular trap formation, and other related processes ([Figure S4B](#)). These findings underscore the strong association between genes involved in inflammatory response and

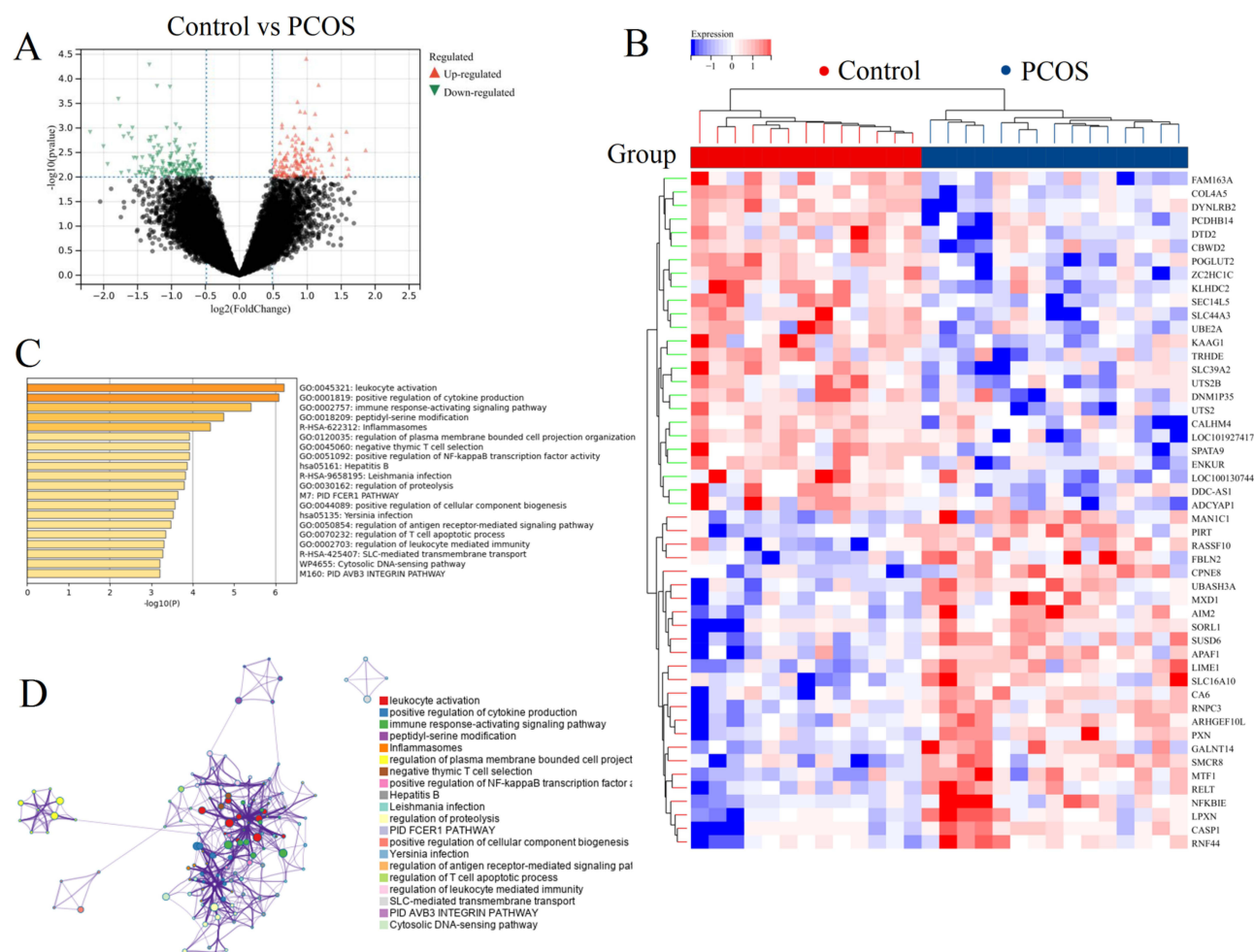


Figure 2 Identification of DEGs and functional enrichment analysis. Volcano (**A**) and heatmap (**B**) diagrams of the DEGs between control and PCOS groups. (**C** and **D**) Functional enrichment analysis for the DEGs.

immune function. Ultimately, topological analysis was utilized to calculate the betweenness centrality, closeness centrality, and degree centrality of 31 nodes (Table S4).

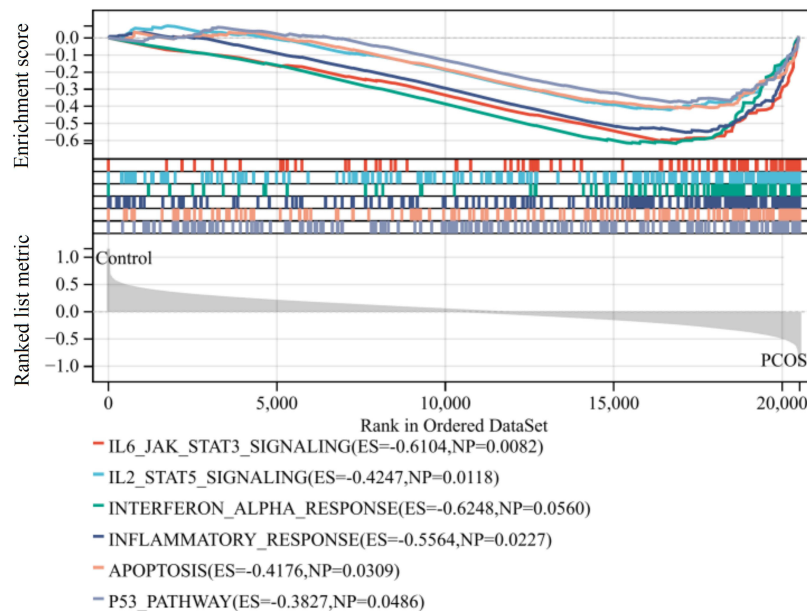
Identification of DEGs in the Hub Modules

As shown in Figure 4A, five important inflammatory response score-related genes (*TGFB2*, *ICAM3*, *WIPF1*, *SLC11A1*, and *NCF2*) were identified from DEGs based on the Venn result. Those genes were significantly up-regulated in the PCOS group ($p < 0.05$) (Figure 4B). In addition, the diagnostic AUC values of *TGFB2*, *ICAM3*, *WIPF1*, *SLC11A1*, and *NCF2* genes were 0.759, 0.831, 0.759, 0.764, and 0.81, respectively (Figure 4C).

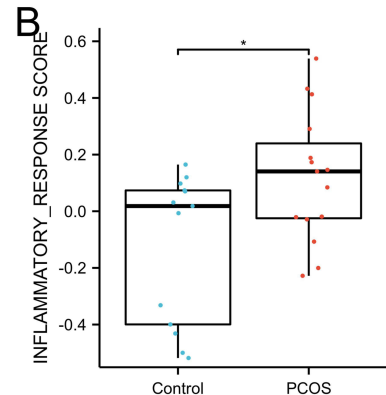
We validated the results by combining the three datasets (GSE137684, GSE80432, and GSE114419 datasets) into one integrated dataset. The expression level of *TGFB2*, *WIPF1*, *SLC11A1*, and *NCF2* genes in the PCOS group was significantly higher than that of the control group ($p < 0.05$). No significant difference in *ICAM3* gene expression between normal and disease groups (Figure 4D). The diagnostic AUC values of *TGFB2*, *ICAM3*, *WIPF1*, *SLC11A1*, and *NCF2* genes were 0.692, 0.647, 0.706, 0.72, and 0.72, respectively (Figure 4E).

The diagnostic performance of a model incorporating the combined assessment of *TGFB2*, *ICAM3*, *WIPF1*, *SLC11A1*, and *NCF2* genes was evaluated using ROC curve analysis. For the training set (Figure S5A), the model demonstrated a considerable ability to distinguish between PCOS patients and controls with an AUC of 0.800, indicating good predictive accuracy. Similarly, the model was assessed in an independent test set to evaluate its generalizability (Figure S5B). The AUC for the test set was 0.772, confirming the model's diagnostic value.

A



B



C



Figure 3 WGCNA identifies the inflammatory response score-related modules. **(A)** GSEA results exhibited the significantly enriched pathways in the HALLMARK set of the PCOS group. **(B)** The inflammatory response score was calculated by GSVA, and the results were presented as box plots. * $p < 0.05$. **(C)** Identification of key modules by WGCNA. The module-trait correlations were presented as a heatmap.

GSEA of Diagnostic Genes

Single gene GSEA was performed to explore the potential signaling pathways associated with these important genes. Notable findings from the GSEA are summarized below. For ICAM3, enrichment was observed in pathways related to acute myeloid leukemia (ES=-0.62, $p < 0.0001$), toll-like receptor signaling (ES=-0.59, $p < 0.0001$), and leukocyte transendothelial migration (ES=-0.48, $p < 0.0001$) (Figure 5A); NCF2 showed significant association with toll-like receptor signaling pathways (ES=-0.57, $p = 0.0037$) and NOD-like receptor signaling pathways (ES=-0.63, $p = 0.0037$), indicating its role in innate immunity (Figure 5B); SLC11A1 was prominently enriched in pathways tied to leukocyte transendothelial migration (ES=-0.49, $p < 0.0001$) and natural killer cell mediated cytotoxicity (ES=-0.60, $p < 0.0001$) (Figure 5C); WIPF1 displayed notable enrichment in alpha-beta T cell activation (ES=-0.59, $p = 0.0102$) and positive

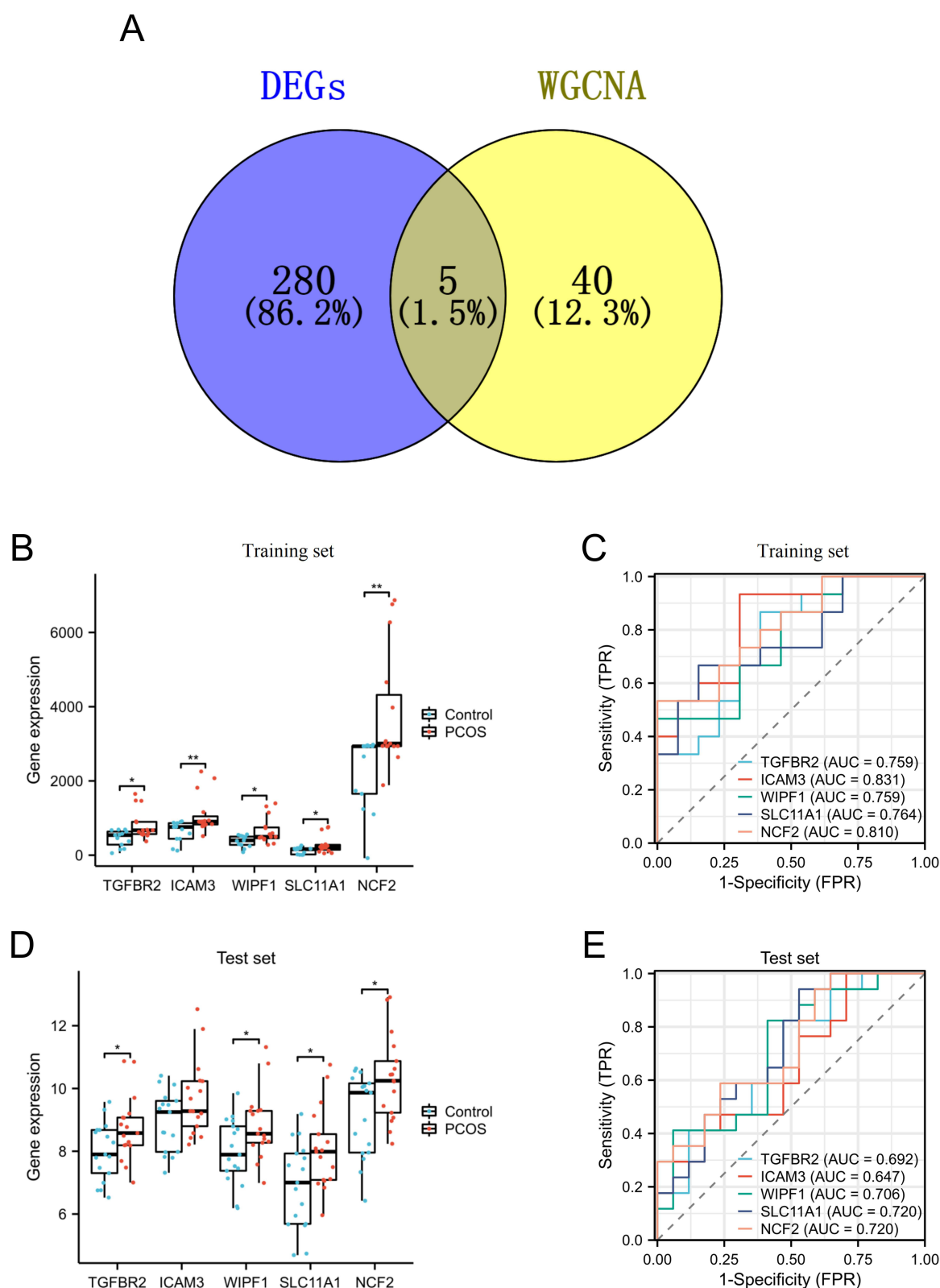


Figure 4 Identification of DEGs in the hub modules. **(A)** The Venn diagram presented the common genes between the DEGs and WGCNA. The gene expression levels **(B)** and ROC curves **(C)** of TGFB2, ICAM3, WIPF1, SLC11A1, and NCF2 genes in the training set **(D)** and test set **(E)**. * $p < 0.05$, ** $p < 0.01$.

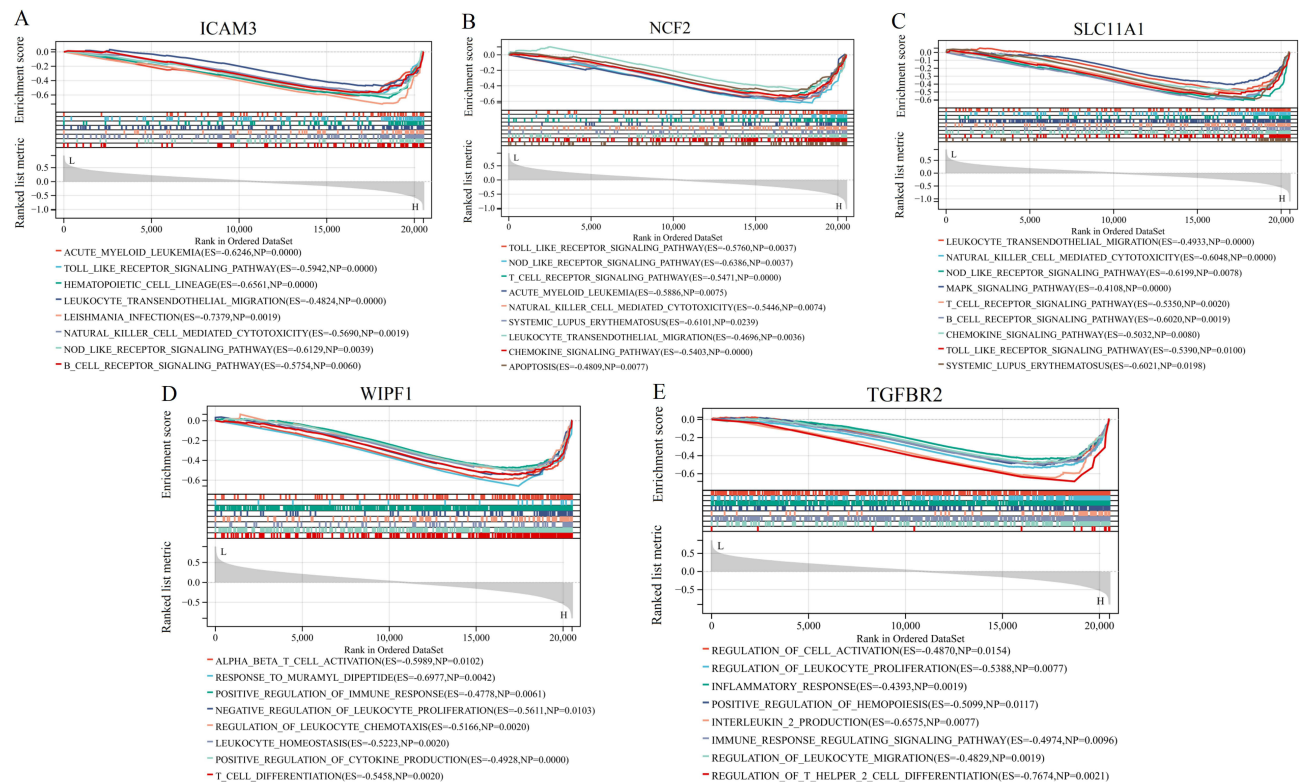


Figure 5 The potential pathways in association with the core genes have been identified by GSEA. The representative pathways were mainly enriched in high expression of ICAM3 (A), NCF2 (B), SLC11A1 (C), WIPF1 (D), and TGFB2 (E).

regulation of immune response (ES=-0.47, $p=0.006$), suggesting its involvement in adaptive immune responses (Figure 5D); TGFB2 enrichment was evident in pathways governing regulation of T-helper 2 cell differentiation (ES=-0.76, $p=0.0021$) and interleukin-2 production (ES=-0.65, $p=0.0077$), reflecting its critical role in immune regulation (Figure 5E). These pathway associations suggest the potential involvement of these genes in the pathophysiology of immune-related disorders.

Unsupervised Cluster Analysis Identifies Inflammation-Related Molecular Subtypes

As shown in Figure 6A, in the training set, two subtypes of PCOS (C1 and C2) were identified based on the expression of five core genes. In addition, we performed differential expression analysis between C1 and C2 subgroups, and a total of 187 DEGs (92 up-regulated genes and 95 down-regulated genes) were identified (Figure 6B and C). As for GO terms, 187 DEGs were mainly enriched in leukocyte migration, chemotaxis, myeloid leukocyte migration, leukocyte chemotaxis, cytokine-mediated signaling pathway, etc (Figure 7A). As shown in Figure 7B, KEGG pathway analysis revealed that these DEGs were significantly enriched in the IL-17 signaling pathway (Figure 8A), viral protein interaction with cytokine and cytokine receptor, chemokine signaling pathway, TNF signaling pathway (Figure 8B), cytokine-cytokine receptor interaction, kaposi sarcoma-associated herpesvirus infection, etc.²⁴ In addition, GSEA results showed that apoptosis, IL6-JAK-STAT3 signaling, IL2-STAT5 signaling, PI3K-AKT-MTOR signaling, TNFA signaling via NFkB, and inflammatory response were mainly enriched in the C2 subgroup (Figure 9A). GSVA results indicated that leukocyte chemotaxis, interferon-gamma response, positive regulation of T cell proliferation, regulation of neutrophil degranulation, positive regulation of lymphocyte differentiation, interleukin 6 production, interferon alpha production, and myeloid cell differentiation were activated in the C2 subgroup (Figure 9B), suggesting that the C2 subgroup had higher immune activation than the C1 subgroup. As shown in Figure 10A, there were remarkable interactions between immune cell populations. In addition, the proportion of T cells CD8 was significantly lower in the C1 group than C2 group, whereas

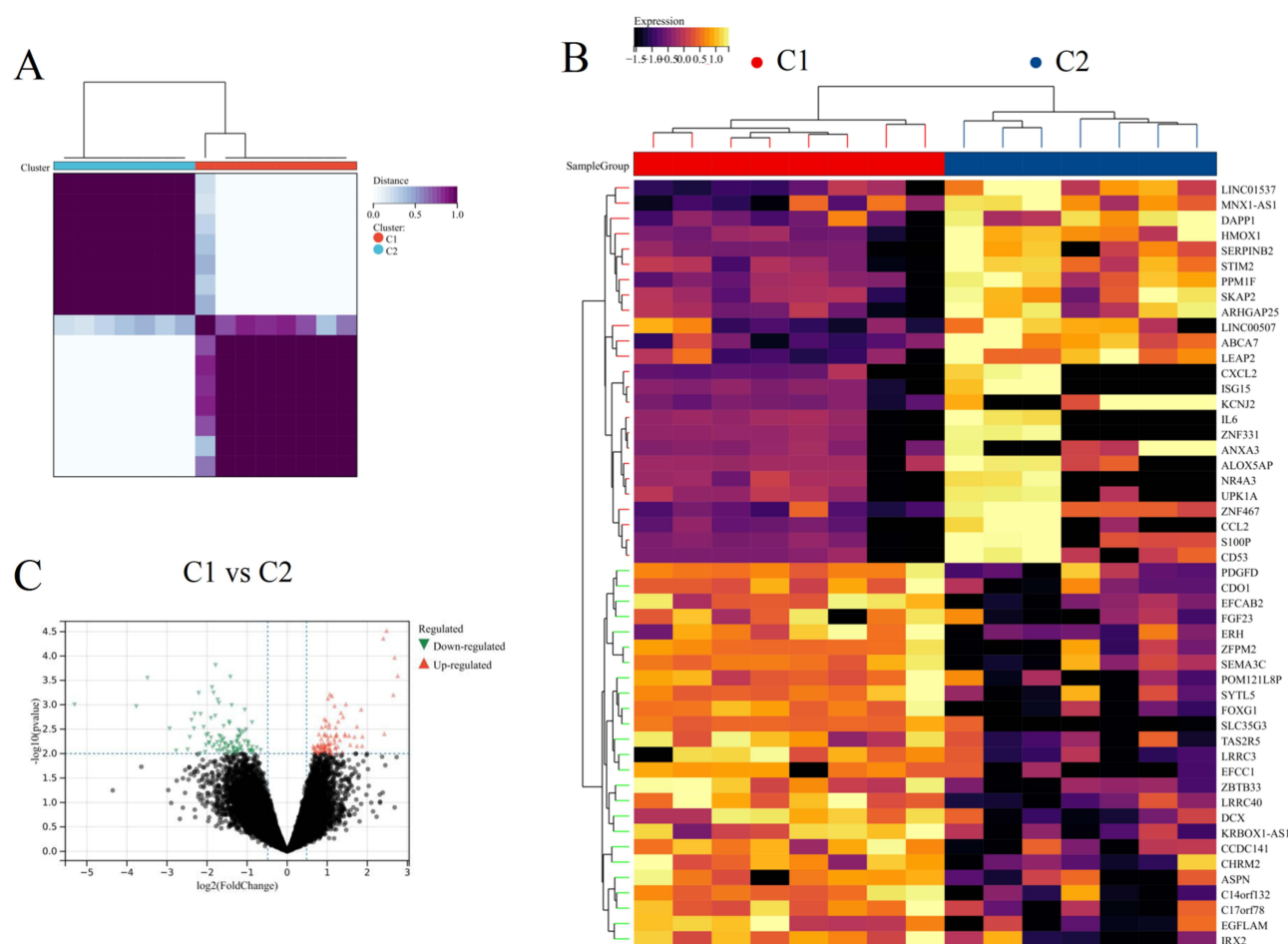


Figure 6 Unsupervised cluster analysis. (A) Consensus clustering matrix when $k = 2$. Heatmap (B) and volcano (C) diagrams of the DEGs between C1 and C2 subgroups.

the proportion of T cells CD4 memory resting and T cells gamma delta was significantly higher in the C1 group than the C2 group (Figure 10B).

Drug Discovery and Molecular Docking Analysis

As shown in Table 2, the top 5 small molecules (esmolol, desoxyepanin, actarit, pentoxifylline, and coumarin) with the highest negative score have been evaluated as possible drugs against PCOS. Figure 11A presented the 2D chemical structure of drug candidates. For molecular docking validation, these five drug candidates and the core inflammation-related proteins (TGFB2, ICAM3, WIPF1, SLC11A1, and NCF2) were selected. Figure 11B presented the binding energy for molecular docking. Of these five small molecules, esmolol had the lowest binding energy to the core target protein. Therefore, we applied PyMOL software to visualize the results of molecular docking (Figure 12A–E). For example, esmolol could bind to TGFB2 and form hydrogen bonds with amino acid residues (GLN-41, ASN-40, and THR-109) in the vicinity of the active site, thereby exerting its therapeutic effects. As a result, we believed that esmolol may be a potential therapeutic drug for the treatment of PCOS that was worthy of further investigation.

Validation of Diagnostic Markers Based on the qRT-PCR Analysis

The control group and PCOS group both consisted of 8 patients each, with detailed characteristics provided in Table S5. In order to validate the bioinformatics analyses mentioned above, we conducted a study to examine the expression levels of the five hub biomarkers in clinical samples that we collected (Figure 13). Employing qRT-PCR, we observed a significant upregulation of *TGFB2*, *ICAM3*, *WIPF1*, *SLC11A1*, and *NCF2* in PCOS patients when compared to the

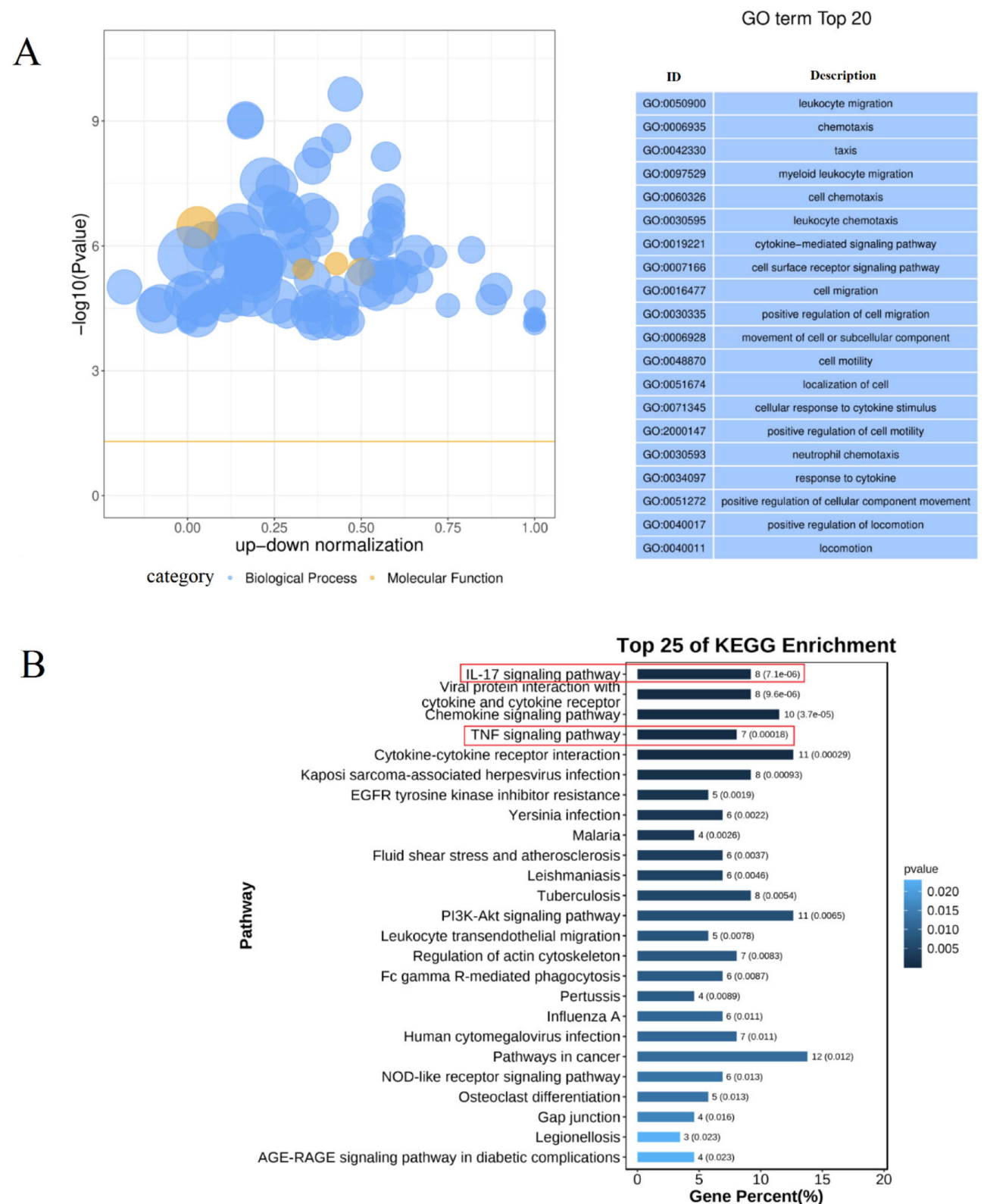


Figure 7 Enrichment analysis of DEGs between the two subgroups. The results of GO (A) and KEGG (B) enrichment analyses.

[illegible]

TNF SIGNALING PATHWAY

Leukocyte recruitment

Ccl2, Ccl5, Ccl20, Ccl1, Ccl2, Ccl3, Ccl5, Ccl10, Cxcl1

Leukocyte activation

Ccl1, Ccl2

Surface receptors

Fas, IL18R1, Jag1

Inflammatory cytokines

IL1b, IL6, IL15, IL17, IL18, IL19, IL20, IL21, IL22, IL23, IL24, IL25, IL26, IL27, IL28, IL29, IL30, IL31, IL32, IL33, IL34, IL35, IL36, IL37, IL38, IL39, IL40, IL41, IL42, IL43, IL44, IL45, IL46, IL47, IL48, IL49, IL50, IL51, IL52, IL53, IL54, IL55, IL56, IL57, IL58, IL59, IL60, IL61, IL62, IL63, IL64, IL65, IL66, IL67, IL68, IL69, IL70, IL71, IL72, IL73, IL74, IL75, IL76, IL77, IL78, IL79, IL80, IL81, IL82, IL83, IL84, IL85, IL86, IL87, IL88, IL89, IL90, IL91, IL92, IL93, IL94, IL95, IL96, IL97, IL98, IL99, IL100, IL101, IL102, IL103, IL104, IL105, IL106, IL107, IL108, IL109, IL110, IL111, IL112, IL113, IL114, IL115, IL116, IL117, IL118, IL119, IL120, IL121, IL122, IL123, IL124, IL125, IL126, IL127, IL128, IL129, IL130, IL131, IL132, IL133, IL134, IL135, IL136, IL137, IL138, IL139, IL140, IL141, IL142, IL143, IL144, IL145, IL146, IL147, IL148, IL149, IL150, IL151, IL152, IL153, IL154, IL155, IL156, IL157, IL158, IL159, IL160, IL161, IL162, IL163, IL164, IL165, IL166, IL167, IL168, IL169, IL170, IL171, IL172, IL173, IL174, IL175, IL176, IL177, IL178, IL179, IL180, IL181, IL182, IL183, IL184, IL185, IL186, IL187, IL188, IL189, IL190, IL191, IL192, IL193, IL194, IL195, IL196, IL197, IL198, IL199, IL200, IL201, IL202, IL203, IL204, IL205, IL206, IL207, IL208, IL209, IL210, IL211, IL212, IL213, IL214, IL215, IL216, IL217, IL218, IL219, IL220, IL221, IL222, IL223, IL224, IL225, IL226, IL227, IL228, IL229, IL230, IL231, IL232, IL233, IL234, IL235, IL236, IL237, IL238, IL239, IL240, IL241, IL242, IL243, IL244, IL245, IL246, IL247, IL248, IL249, IL250, IL251, IL252, IL253, IL254, IL255, IL256, IL257, IL258, IL259, IL260, IL261, IL262, IL263, IL264, IL265, IL266, IL267, IL268, IL269, IL270, IL271, IL272, IL273, IL274, IL275, IL276, IL277, IL278, IL279, IL280, IL281, IL282, IL283, IL284, IL285, IL286, IL287, IL288, IL289, IL290, IL291, IL292, IL293, IL294, IL295, IL296, IL297, IL298, IL299, IL300, IL301, IL302, IL303, IL304, IL305, IL306, IL307, IL308, IL309, IL310, IL311, IL312, IL313, IL314, IL315, IL316, IL317, IL318, IL319, IL320, IL321, IL322, IL323, IL324, IL325, IL326, IL327, IL328, IL329, IL330, IL331, IL332, IL333, IL334, IL335, IL336, IL337, IL338, IL339, IL340, IL341, IL342, IL343, IL344, IL345, IL346, IL347, IL348, IL349, IL350, IL351, IL352, IL353, IL354, IL355, IL356, IL357, IL358, IL359, IL360, IL361, IL362, IL363, IL364, IL365, IL366, IL367, IL368, IL369, IL370, IL371, IL372, IL373, IL374, IL375, IL376, IL377, IL378, IL379, IL380, IL381, IL382, IL383, IL384, IL385, IL386, IL387, IL388, IL389, IL390, IL391, IL392, IL393, IL394, IL395, IL396, IL397, IL398, IL399, IL400, IL401, IL402, IL403, IL404, IL405, IL406, IL407, IL408, IL409, IL410, IL411, IL412, IL413, IL414, IL415, IL416, IL417, IL418, IL419, IL420, IL421, IL422, IL423, IL424, IL425, IL426, IL427, IL428, IL429, IL430, IL431, IL432, IL433, IL434, IL435, IL436, IL437, IL438, IL439, IL440, IL441, IL442, IL443, IL444, IL445, IL446, IL447, IL448, IL449, IL450, IL451, IL452, IL453, IL454, IL455, IL456, IL457, IL458, IL459, IL460, IL461, IL462, IL463, IL464, IL465, IL466, IL467, IL468, IL469, IL470, IL471, IL472, IL473, IL474, IL475, IL476, IL477, IL478, IL479, IL480, IL481, IL482, IL483, IL484, IL485, IL486, IL487, IL488, IL489, IL490, IL491, IL492, IL493, IL494, IL495, IL496, IL497, IL498, IL499, IL500, IL501, IL502, IL503, IL504, IL505, IL506, IL507, IL508, IL509, IL510, IL511, IL512, IL513, IL514, IL515, IL516, IL517, IL518, IL519, IL520, IL521, IL522, IL523, IL524, IL525, IL526, IL527, IL528, IL529, IL530, IL531, IL532, IL533, IL534, IL535, IL536, IL537, IL538, IL539, IL540, IL541, IL542, IL543, IL544, IL545, IL546, IL547, IL548, IL549, IL550, IL551, IL552, IL553, IL554, IL555, IL556, IL557, IL558, IL559, IL560, IL561, IL562, IL563, IL564, IL565, IL566, IL567, IL568, IL569, IL570, IL571, IL572, IL573, IL574, IL575, IL576, IL577, IL578, IL579, IL580, IL581, IL582, IL583, IL584, IL585, IL586, IL587, IL588, IL589, IL590, IL591, IL592, IL593, IL594, IL595, IL596, IL597, IL598, IL599, IL600, IL601, IL602, IL603, IL604, IL605, IL606, IL607, IL608, IL609, IL610, IL611, IL612, IL613, IL614, IL615, IL616, IL617, IL618, IL619, IL620, IL621, IL622, IL623, IL624, IL625, IL626, IL627, IL628, IL629, IL630, IL631, IL632, IL633, IL634, IL635, IL636, IL637, IL638, IL639, IL640, IL641, IL642, IL643, IL644, IL645, IL646, IL647, IL648, IL649, IL650, IL651, IL652, IL653, IL654, IL655, IL656, IL657, IL658, IL659, IL660, IL661, IL662, IL663, IL664, IL665, IL666, IL667, IL668, IL669, IL670, IL671, IL672, IL673, IL674, IL675, IL676, IL677, IL678, IL679, IL680, IL681, IL682, IL683, IL684, IL685, IL686, IL687, IL688, IL689, IL690, IL691, IL692, IL693, IL694, IL695, IL696, IL697, IL698, IL699, IL700, IL701, IL702, IL703, IL704, IL705, IL706, IL707, IL708, IL709, IL710, IL711, IL712, IL713, IL714, IL715, IL716, IL717, IL718, IL719, IL720, IL721, IL722, IL723, IL724, IL725, IL726, IL727, IL728, IL729, IL730, IL731, IL732, IL733, IL734, IL735, IL736, IL737, IL738, IL739, IL740, IL741, IL742, IL743, IL744, IL745, IL746, IL747, IL748, IL749, IL750, IL751, IL752, IL753, IL754, IL755, IL756, IL757, IL758, IL759, IL760, IL761, IL762, IL763, IL764, IL765, IL766, IL767, IL768, IL769,

4712 <https://doi.org/10.2147/JIR.S460437>
DovePress

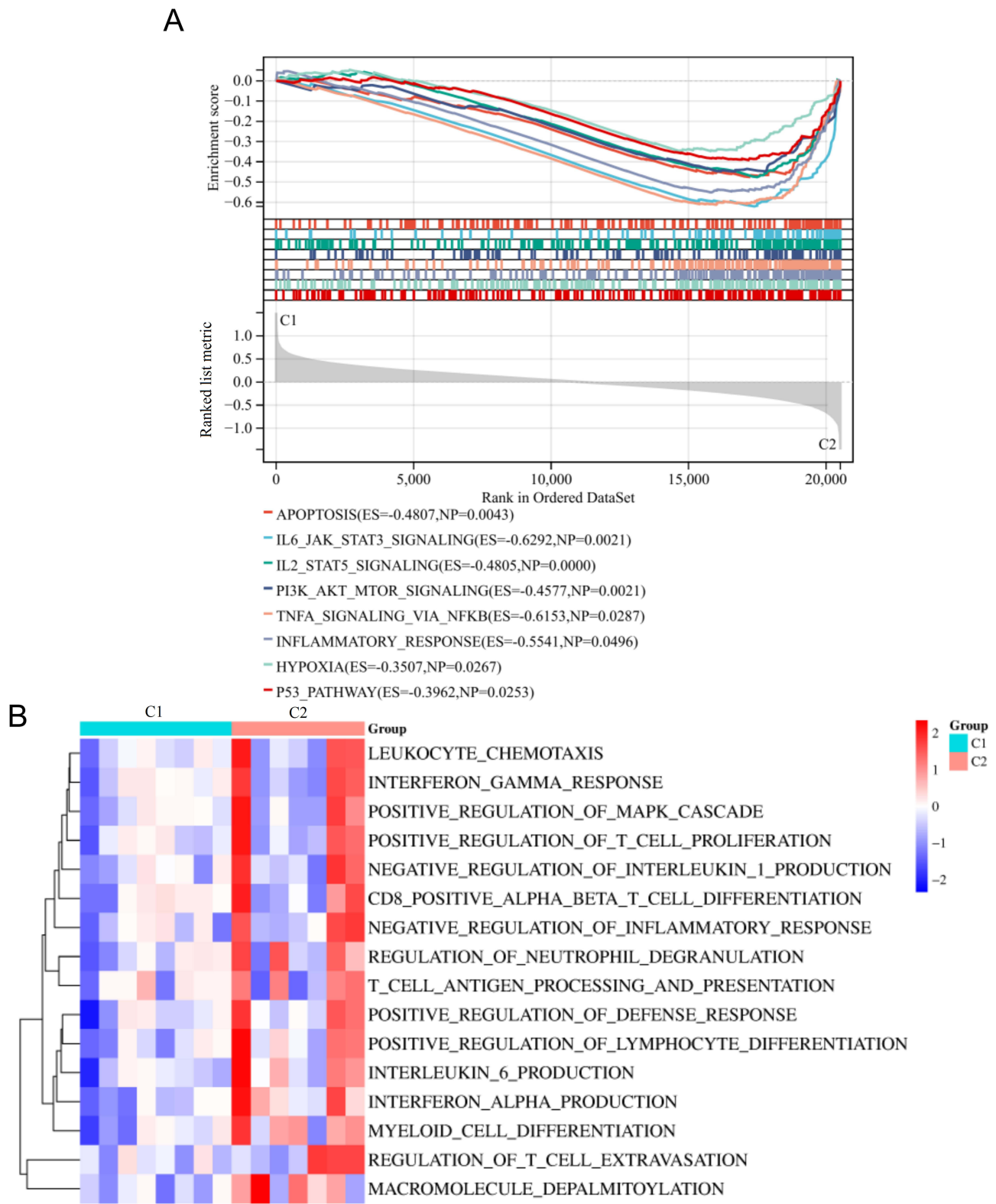
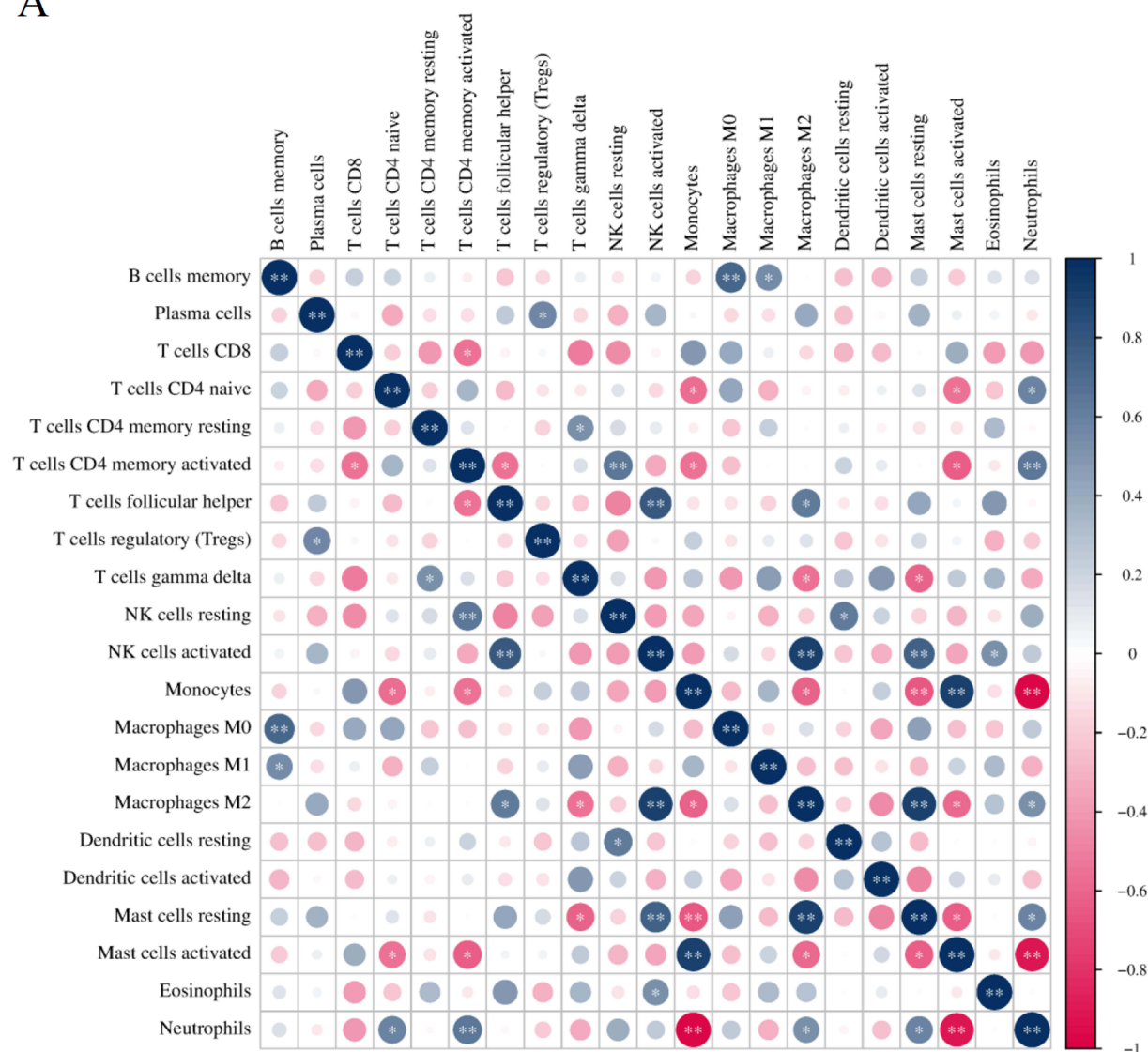


Figure 9 GSEA (A) and GSVA (B) were performed to explore the potential pathways between the C1 and C2 subgroups.

A



B

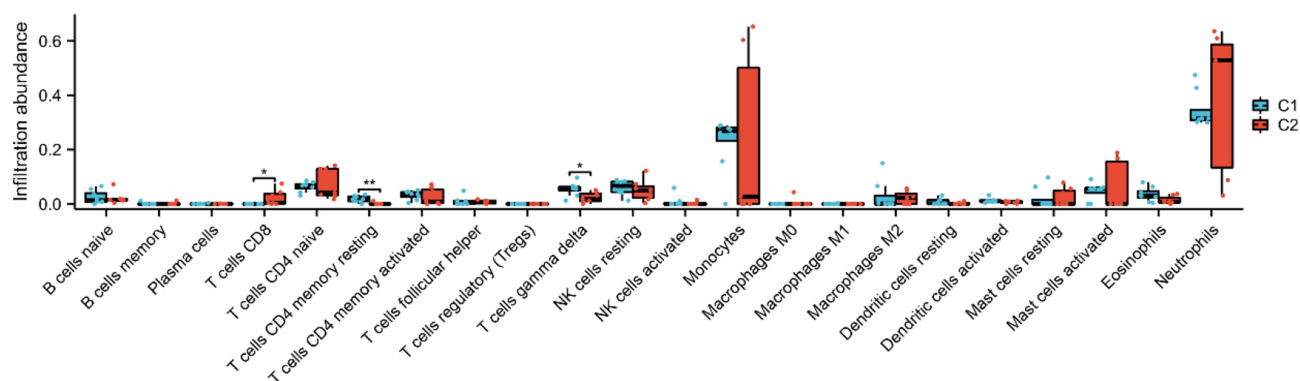


Figure 10 Immune cell infiltration analysis of molecular subtypes. (A) The correlation analysis of the immune cells. (B) The landscape of the immune cells between C1 and C2 subgroups. * $p < 0.05$, ** $p < 0.01$.

Table 2 Results of CMap Analysis

Rank	Score	Name	Description
1	-99.93	Esmolol	Adrenergic receptor antagonist
2	-99.93	Desoxypeganine	Acetylcholinesterase inhibitor
3	-99.89	Actarit	Interleukin receptor agonist
4	-99.68	Pentoxifylline	Phosphodiesterase inhibitor
5	-99.68	Coumarin	Vitamin K antagonist

control group ($p < 0.05$ or $p < 0.01$ or $p < 0.001$). These findings were consistent with the results obtained from our bioinformatics analysis. In addition, the correlation analysis demonstrated significant associations between the levels of luteinizing hormone (LH) and testosterone (T) with the expression of key inflammatory-related genes. The data depicted in [Figure S6](#) shows that both LH and T levels were positively correlated with the gene expression levels of *TGFBR2*, *ICAM3*, *WIPF1*, *SLC11A1*, and *NCF2*. The observed correlations emphasize the potential link between inflammation and hormone levels in the clinical context, thus providing insights into the underlying molecular interactions in PCOS.

Discussion

PCOS is a complex endocrine disorder that has adverse effects on both the reproductive and metabolic functions of women.²⁵ Unfortunately, the specific pathogenesis of PCOS is poorly understood from available epidemiological and basic research.²⁶ As there are no effective diagnostic indicators in clinical practice, it is often the case that patients with PCOS miss the right time for diagnosis and treatment. Recent studies have indicated that a key factor in the pathogenesis of PCOS is chronic low-grade inflammation.^{11,27} In addition, dysregulation of inflammatory response genes in PCOS was identified by peripheral blood transcriptomics.²⁸ In our study, PCOS patients had significantly higher inflammatory response scores compared to the normal group, which is consistent with previous studies. Thus, the identification of specific diagnostic markers and analysis of genes that are associated with the inflammatory response in PCOS are

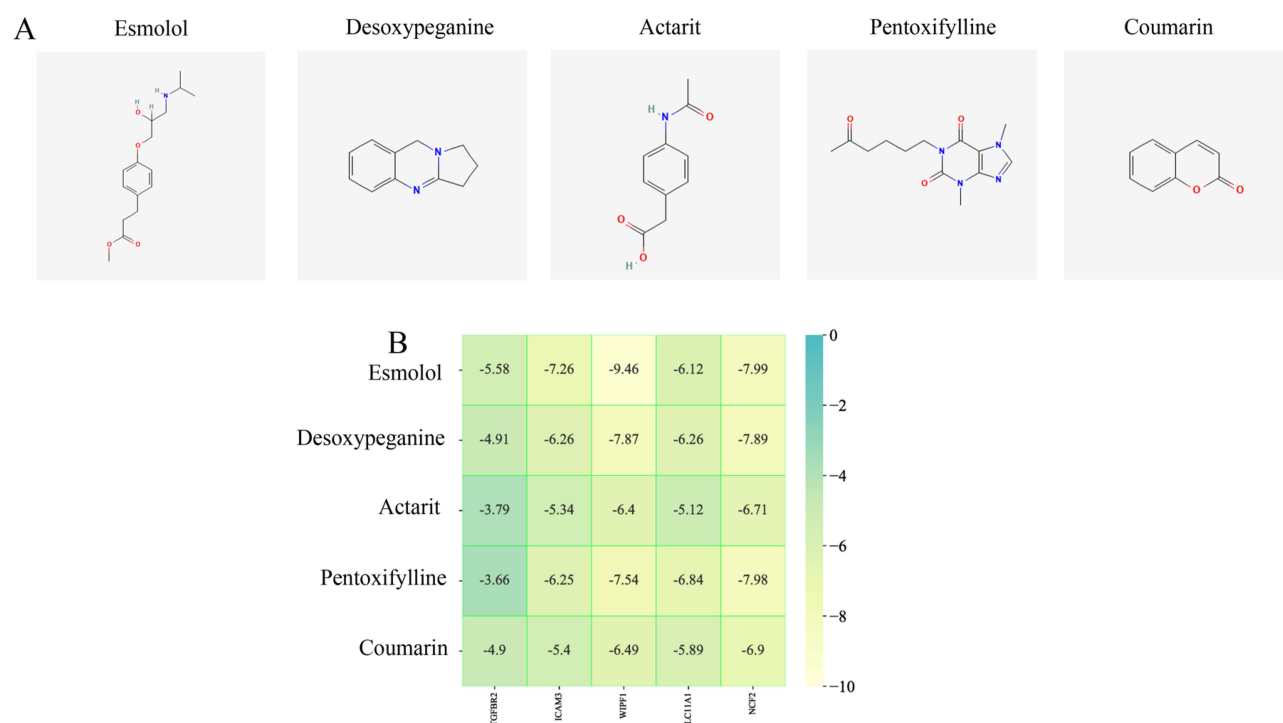


Figure 11 Screening and validation of potential drugs for PCOS patients. **(A)** Chemical structure of the potential small molecule compounds. **(B)** The lowest binding energy for molecular docking.

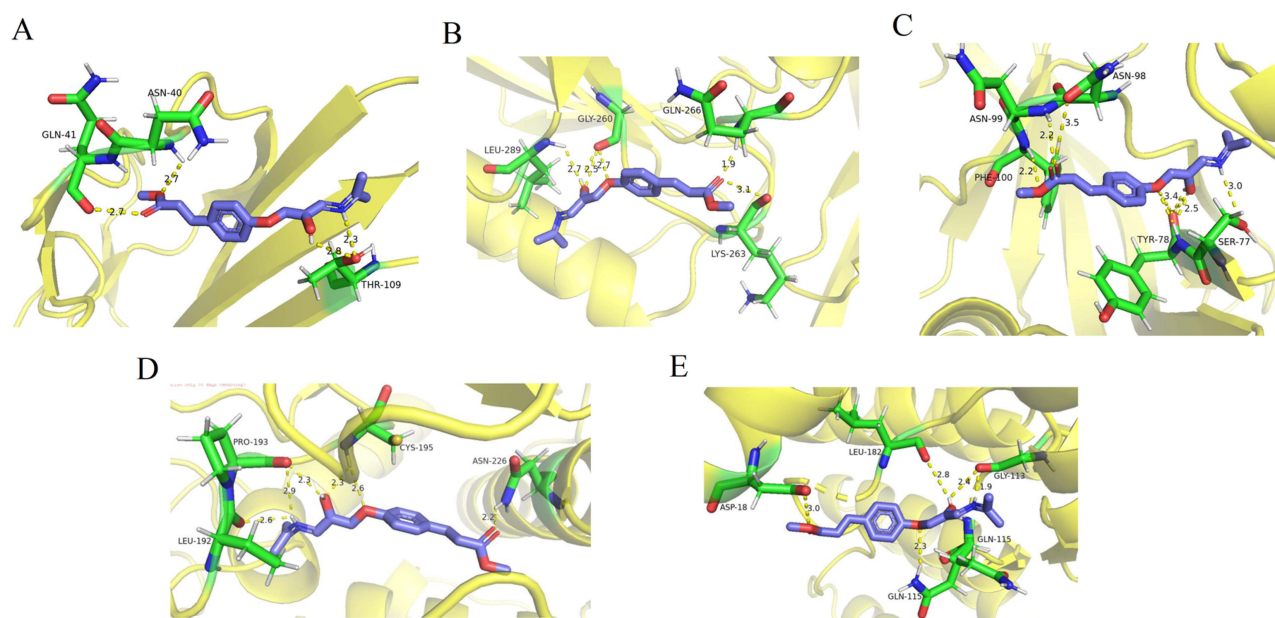


Figure 12 Molecular docking results of esmolol with hub targets. (A) esmolol-TGFB2. (B) esmolol-ICAM3. (C) esmolol-WIPF1. (D) esmolol-SLC11A1. (E) esmolol-NCF2.

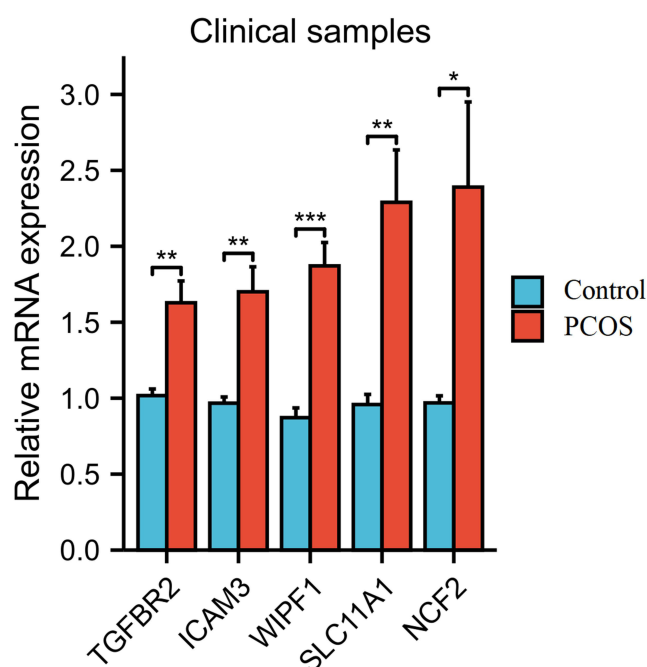


Figure 13 Clinical samples are collected to validate the accuracy and reliability of diagnostic markers. * $p < 0.05$, ** $p < 0.01$, *** $p < 0.001$.

important. In our study, enrichment analysis results revealed that DEGs were found to be involved in inflammation- and immune-related pathways. We attempted to identify diagnostic markers of PCOS using WGCNA analysis of genes related to the inflammatory response score. In addition, potential therapeutic drugs for PCOS were screened through CMap analysis.

In our study, we identified five characteristic genes (*TGFB2*, *ICAM3*, *WIPF1*, *SLC11A1*, and *NCF2*) that could be considered diagnostic markers for PCOS in both training and test sets. The TGF-beta superfamily played an important

role in human ovarian and placental function.²⁹ It is becoming more and more apparent that the TGF- β -signaling pathway is significantly involved in the progression of PCOS.³⁰ Inhibition of TGF-beta signaling may be part of the pathogenesis of PCOS.³¹ The TGF- β 1/Smad3 signaling pathway has been linked to the inhibition of the growth of ovarian follicles in individuals with PCOS by controlling the programmed cell death of granulosa cells.³² The maintenance of *TGFBR2* through USP9X resulted in the activation of the TGF-beta pathway, which further inhibited granulosa cell apoptosis.³³ In addition, the expression of *TGFBR2* was higher in the granulosa cells of cows with ACTH-induced cystic ovarian disease than in controls.³⁴ Noticeable rise in the levels of *TGFBR2* expression was observed in normo-androgenic PCOS individuals when compared to the control group.³⁵ ICAM family members played a vital role in immune responses, inflammation, and intracellular signaling.³⁶ *ICAM3* has been implicated in T lymphocyte activation and immune cell interactions in several studies.^{37,38} *SLC11A1* had multiple effects on macrophage function.³⁹ Previous studies have indicated that *SLC11A1* is implicated in the acute inflammatory response in pristane-induced arthritis.^{40,41} Several studies indicated that changes in the *NCF2* gene sequence may be associated with the development of inflammatory bowel disease, lupus, and coeliac disease.^{42,43} *WIPF1* was involved in organizing and polymerizing the actin cytoskeleton, which was linked to cell invasion and proliferation.⁴⁴ However, no relevant studies reported on the role of *ICAM3*, *WIPF1*, *SLC11A1*, and *NCF2* in PCOS progression. In this study, for the first time, our results indicated that *ICAM3*, *WIPF1*, *SLC11A1*, and *NCF2* were increased in PCOS and could act as diagnostic markers for PCOS patients.

PCOS is a low-level chronic inflammation.⁴⁵ A previous research findings suggest significant changes in the immune system within the ovaries of individuals with PCOS.⁴⁶ A recent investigation revealed that PCOS patients exhibit elevated levels of inflammatory markers, heightened levels of reactive oxygen species, and disrupted mitochondrial function in their granulosa cells.⁴⁷ IL molecules, including IL-17A, IL-23, and IL-33, played a vital role in the pathogenesis of PCOS.⁴⁸ Patients with PCOS have elevated levels of TNF- α in serum and endometrial fluid.⁴⁹ In addition, the Th17/Treg cell imbalance in favor of pro-inflammatory Th17 cells has been implicated in the pathogenesis of PCOS patients with autoimmune thyroiditis.⁵⁰

In the present study, consensus clustering was performed to identify two inflammation-related patterns (C1 and C2). Functional enrichment analysis indicated these DEGs between C1 and C2 subgroups were significantly enriched in the IL-17 signaling pathway and TNF signaling pathway. In addition, the results of GSVA, GSEA, and immune cell infiltration revealed that there was significant heterogeneity between the two subtypes and that the immune- and inflammation-related pathways in the two subtypes were different. Notably, the C2 subtype exhibited activated immune- and inflammation-related pathways (including PI3K-AKT-MTOR signaling, TNFA signaling via NFkB, inflammatory response, positive regulation of T cell proliferation, etc). Thus, we speculated that the C2 subgroup was more likely to have advanced PCOS than the C1 subgroup.

However, our study has certain limitations. Although we confirmed the expression levels of diagnostic genes with clinical samples, further enhancing the reliability of the results would necessitate a broader array of clinical samples. Due to sample size limitations in the GEO database, we propose that future research should consider stratifying PCOS patients by subtype to further clarify the specific inflammatory pathways involved in different PCOS categories.

Conclusion

In Conclusion, our findings highlighted the vital role of the inflammatory response in the pathogenesis of PCOS and suggested that the five core genes identified in this study could be used to diagnose and treat PCOS patients. In addition, we have proposed a new molecular classification that included both non-inflammation and inflammation subgroups of patients with PCOS. Our research could provide theoretical guidance for further elucidation of the pathogenesis of PCOS and directions for drug screening and individualized treatment of PCOS.

Data Sharing Statement

All data used in the present study were available from the GEO database (<https://www.ncbi.nlm.nih.gov/geo/>). The accession numbers are as follows: GSE102293, GSE34526, GSE5850, GSE137684, GSE80432, and GSE114419).

Ethics Approval and Consent to Participate

This study was approved by the Ethics Committee of the Second Affiliated Hospital of Shandong First Medical University and was conducted in adherence to the Declaration of Helsinki. Consent for participation was acquired from all individuals.

Funding

This work was supported by the Natural Science Foundation of Shandong Province of China (Grant No. ZR2017LH023); Higher Educational Science and Technology Program of Shandong Province, China (Grant No. J17KA246); Shandong Provincial Key Laboratory of Endocrinology and Lipid Metabolism (Grant No. SDkeylab-Endo&LiMe2019-01); Medical as well as Academic Promotion Program of Shandong First Medical University (Grant No. 2019QL017).

Disclosure

The authors report no conflicts of interest in this work.

References

- Meier RK. Polycystic ovary syndrome. *Nurs Clin North Am*. 2018;53(3):407–420. doi:10.1016/j.cnur.2018.04.008
- Sirmans SM, Pate KA. Epidemiology, diagnosis, and management of polycystic ovary syndrome. *Clin Epidemiol*. 2013;6:1–13. doi:10.2147/CLEPS.37559
- Barthelmess EK, Naz RK. Polycystic ovary syndrome: current status and future perspective. *Front Biosci*. 2014;6:104–119.
- Ehrmann DA. Polycystic Ovary Syndrome. *N Engl J Med*. 2005;352(12):1223–1236. doi:10.1056/NEJMra041536
- Christ JP, Falcone T. Bariatric surgery improves hyperandrogenism, menstrual irregularities, and metabolic dysfunction among Women with Polycystic Ovary Syndrome (PCOS). *Obes Surg*. 2018;28(8):2171–2177. doi:10.1007/s11695-018-3155-6
- Escobar-Morreale HF. Polycystic ovary syndrome: definition, aetiology, diagnosis and treatment. *Nat Rev Endocrinol*. 2018;14(5):270–284. doi:10.1038/nrendo.2018.24
- Walters KA, Gilchrist RB, Ledger WL, Teede HJ, Handelsman DJ, Campbell RE. New perspectives on the pathogenesis of PCOS: neuroendocrine origins. *Trends Endocrinol Metab*. 2018;29(12):841–852. doi:10.1016/j.tem.2018.08.005
- Duffy DM, Ko C, Jo M, Brannstrom M, Curry TE. Ovulation: parallels with inflammatory processes. *Endocrine Rev*. 2019;40(2):369–416. doi:10.1210/er.2018-00075
- Deligeorgoglou E, Vrachnis N, Athanasopoulos N, et al. Mediators of chronic inflammation in polycystic ovarian syndrome. *Gynecological Endocrinol*. 2012;28(12):974–978. doi:10.3109/09513590.2012.683082
- Sanchez-Garrido MA, Tena-Sempere M. Metabolic dysfunction in polycystic ovary syndrome: pathogenic role of androgen excess and potential therapeutic strategies. *Mol Metabol*. 2020;35:100937. doi:10.1016/j.molmet.2020.01.001
- Zhai Y, Pang Y. Systemic and ovarian inflammation in women with polycystic ovary syndrome. *J Reprod Immunol*. 2022;151:103628. doi:10.1016/j.jri.2022.103628
- González F, Rote NS, Minium J, Kirwan JP. Increased activation of nuclear factor kappaB triggers inflammation and insulin resistance in polycystic ovary syndrome. *J Clin Endocrinol Metab*. 2006;91(4):1508–1512. doi:10.1210/jc.2005-2327
- Koc O, Ozdemirici S, Acet M, Soyuturk U, Aydin S. Nuclear factor-κB expression in the endometrium of normal and overweight women with polycystic ovary syndrome. *J Obstetrics Gynaecol*. 2017;37(7):924–930. doi:10.1080/01443615.2017.1315563
- González F, Considine RV, Abdelhadi OA, Acton AJ. Inflammation triggered by saturated fat ingestion is linked to insulin resistance and hyperandrogenism in polycystic ovary syndrome. *J Clin Endocrinol Metab*. 2020;105(6):e2152–e2167. doi:10.1210/clinem/dgaa108
- Zhou Y, Zhou B, Pache L, et al. Metascape provides a biologist-oriented resource for the analysis of systems-level datasets. *Nat Commun*. 2019;10(1):1523. doi:10.1038/s41467-019-09234-6
- Powers RK, Goodspeed A, Pielke-Lombardo H, Tan AC, Costello JC. GSEA-InContext: identifying novel and common patterns in expression experiments. *Bioinformatics*. 2018;34(13):i555–i564. doi:10.1093/bioinformatics/bty271
- Szklarczyk D, Gable AL, Nastou KC, et al. The STRING database in 2021: customizable protein-protein networks, and functional characterization of user-uploaded gene/measurement sets. *Nucleic Acids Res*. 2021;49(D1):D605–D612. doi:10.1093/nar/gkaa1074
- Shannon P, Markiel A, Ozier O, et al. Cytoscape: a software environment for integrated models of biomolecular interaction networks. *Genome Res*. 2003;13(11):2498–2504. doi:10.1101/gr.1239303
- Newman AM, Liu CL, Green MR, et al. Robust enumeration of cell subsets from tissue expression profiles. *Nature Methods*. 2015;12(5):453–457. doi:10.1038/nmeth.3337
- Azziz R. Diagnostic criteria for polycystic ovary syndrome: a reappraisal. *Fertil Sterility*. 2005;83(5):1343–1346. doi:10.1016/j.fertnstert.2005.01.085
- Lamb J, Crawford ED, Peck D, et al. The Connectivity Map: using gene-expression signatures to connect small molecules, genes, and disease. *Science*. 2006;313(5795):1929–1935. doi:10.1126/science.1132939
- Subramanian A, Narayan R, Corsello SM, et al. A next generation connectivity map: 11000 platform and the first 1,000,000 profiles. *Cell*. 2017;171(6):1437–1452.e17. doi:10.1016/j.cell.2017.10.049
- Jiang Y, Chen L, Chao Z, Chen T, Zhou Y. Ferroptosis related genes in ischemic and idiopathic cardiomyopathy: screening for potential pharmacological targets. *Front Cell Develop Biol*. 2022;10:817819. doi:10.3389/fcell.2022.817819
- Kanehisa M, Goto S. KEGG: Kyoto Encyclopedia of Genes and Genomes. *Nucleic Acids Res*. 2000;28(1):27–30. doi:10.1093/nar/28.1.27
- Dumesic DA, Oberfield SE, Stener-Victorin E, Marshall JC, Laven JS, Legro RS. Scientific statement on the diagnostic criteria, epidemiology, pathophysiology, and molecular genetics of polycystic ovary syndrome. *Endocrine Rev*. 2015;36(5):487–525. doi:10.1210/er.2015-1018

26. Lizneva D, Suturina L, Walker W, Brakta S, Gavrilova-Jordan L, Azziz R. Criteria, prevalence, and phenotypes of polycystic ovary syndrome. *Fertil Sterility*. 2016;106(1):6–15. doi:10.1016/j.fertnstert.2016.05.003
27. González F. Inflammation in Polycystic Ovary Syndrome: underpinning of insulin resistance and ovarian dysfunction. *Steroids*. 2012;77(4):300–305. doi:10.1016/j.steroids.2011.12.003
28. Su NJ, Ma J, Feng DF, et al. The peripheral blood transcriptome identifies dysregulation of inflammatory response genes in polycystic ovary syndrome. *Gynecological Endocrinol*. 2018;34(7):584–588. doi:10.1080/09513590.2017.1418851
29. Peng C. The TGF-beta superfamily and its roles in the human ovary and placenta. *J Obstet Gynaecology Canada*. 2003;25(10):834–844. doi:10.1016/S1701-2163(16)30674-0
30. Raja-Khan N, Urbanek M, Rodgers RJ, Legro RS. The role of TGF- β in polycystic ovary syndrome. *Reprod Sci*. 2014;21(1):20–31. doi:10.1177/1933719113485294
31. Azumah R, Liu M, Hummitzsch K, et al. Candidate genes for polycystic ovary syndrome are regulated by TGF β in the bovine foetal ovary. *Hum Reprod*. 2022;37(6):1244–1254. doi:10.1093/humrep/deac049
32. Shen H, Wang Y. Activation of TGF- β 1/Smad3 signaling pathway inhibits the development of ovarian follicle in polycystic ovary syndrome by promoting apoptosis of granulosa cells. *J Cell Physiol*. 2019;234(7):11976–11985. doi:10.1002/jcp.27854
33. Yang L, Wang S, Pan Z, Du X, Li Q. TGFBR2 is a novel substrate and indirect transcription target of deubiquitylase USP9X in granulosa cells. *J Cell Physiol*. 2022;237(7):2969–2979. doi:10.1002/jcp.30776
34. Matiller V, Hein GJ, Stassi AF, et al. Expression of TGFBR1, TGFBR2, TGFBR3, ACVR1B and ACVR2B is altered in ovaries of cows with cystic ovarian disease. *Reproduct Domestic Animals*. 2019;54(1):46–54. doi:10.1111/rda.13312
35. Naji M, Aleyasin A, Nekoonam S, Arefian E, Mahdian R, Amidi F. Differential expression of miR-93 and miR-21 in granulosa cells and follicular fluid of polycystic ovary syndrome associating with different phenotypes. *Sci Rep*. 2017;7(1):14671. doi:10.1038/s41598-017-13250-1
36. Xiao X, Mruk DD, Cheng CY. Intercellular adhesion molecules (ICAMs) and spermatogenesis. *Human Reprod Update*. 2013;19(2):167–186. doi:10.1093/humupd/dms049
37. Estechea A, Aguilera-Montilla N, Sánchez-Mateos P, Puig-Kröger A, Langmann T. RUNX3 regulates intercellular adhesion molecule 3 (ICAM-3) expression during macrophage differentiation and monocyte extravasation. *PLoS One*. 2012;7(3):e33313. doi:10.1371/journal.pone.0033313
38. Montoya MC, Sancho D, Bonello G, et al. Role of ICAM-3 in the initial interaction of T lymphocytes and APCs. *Nat Immunol*. 2002;3(2):159–168. doi:10.1038/ni753
39. Wyllie S, Seu P, Goss JA. The natural resistance-associated macrophage protein 1 Slc11a1 (formerly Nramp1) and iron metabolism in macrophages. *Microb Infect*. 2002;4(3):351–359. doi:10.1016/S1286-4579(02)01548-4
40. Correa MA, Canhamero T, Borrego A, et al. Slc11a1 (Nramp-1) gene modulates immune-inflammation genes in macrophages during pristane-induced arthritis in mice. *Inflammation Res*. 2017;66(11):969–980. doi:10.1007/s00011-017-1077-8
41. Peters LC, Jensen JR, Borrego A, et al. Slc11a1 (formerly NRAMP1) gene modulates both acute inflammatory reactions and pristane-induced arthritis in mice. *Genes Immun*. 2007;8(1):51–56. doi:10.1038/sj.gene.6364358
42. O'Neill S, Brault J, Stasia MJ, Knaus UG. Genetic disorders coupled to ROS deficiency. *Redox Biol*. 2015;6:135–156. doi:10.1016/j.redox.2015.07.009
43. Bakutenko IY, Haurlychky ID, Nikitchenko NV, et al. Neutrophil cytosolic factor 2 (NCF2) gene polymorphism is associated with juvenile-onset systemic lupus erythematosus, but probably not with other autoimmune rheumatic diseases in children. *Mol Genet Genomic Med*. 2022;10(1):e1859. doi:10.1002/mggg.1859
44. Donnelly SK, Weisswange I, Zettl M, Way M. WIP provides an essential link between Nck and N-WASP during Arp2/3-dependent actin polymerization. *Curr Biol*. 2013;23(11):999–1006. doi:10.1016/j.cub.2013.04.051
45. Zafari Zangeneh F, Naghizadeh MM, Masoumi M. Polycystic ovary syndrome and circulating inflammatory markers. *Int J Reprod BioMed*. 2017;15(6):375–382.
46. Schmidt J, Weijdegård B, Mikkelsen AL, Lindenberg S, Nilsson L, Brännström M. Differential expression of inflammation-related genes in the ovarian stroma and granulosa cells of PCOS women. *Mol Hum Reprod*. 2014;20(1):49–58. doi:10.1093/molehr/gat051
47. Wang Y, Yang Q, Wang H, et al. NAD⁺ deficiency and mitochondrial dysfunction in granulosa cells of women with polycystic ovary syndrome. *Biol Reprod*. 2021;105(2):371–380. doi:10.1093/biolre/ioab078
48. Karakose M, Demircan K, Tural E, et al. Clinical significance of ADAMTS1, ADAMTS5, ADAMTS9 aggrecanases and IL-17A, IL-23, IL-33 cytokines in polycystic ovary syndrome. *J Endocrinol Invest*. 2016;39(11):1269–1275. doi:10.1007/s40618-016-0472-2
49. Ha LX, Li WX, Du YD, Yuan YY, Qu XX. Tumor necrosis factor alpha level in the uterine fluid of patients with polycystic ovary syndrome and its correlation with clinical parameters. *J Inflamm Res*. 2022;15:6015–6020. doi:10.2147/JIR.S382808
50. Ma M, Wang M, Xu F, Hao S. The imbalance in Th17 and treg cells in polycystic ovary syndrome patients with autoimmune thyroiditis. *Immunol Invest*. 2022;51(5):1170–1181. doi:10.1080/08820139.2021.1915329